Comparison of two models to calculate the period of compound pendulum with liquid damping

WANG JINTIAN, 6597, GUANGHUA CAMBRIDGE INTERNATIONAL SCHOOL

Contents

Abstract

This study explores two models for calculating the oscillation period of a compound pendulum affected by liquid damping. Theoretical derivations provide expressions for corrected periods, with one model assuming the damping force is directly proportional to velocity, and the other assuming it is proportional to the square of velocity. Experiments confirm the feasibility of small-angle approximations and investigate the relationship between rotation radius and period. Theoretical analysis using Python demonstrates the reliability of both models under a small radius of rotation of the mass center. Considering the computational complexity, the essay recommends the linear model for small radii and favors the squared model for larger radii when calculating period approximately.

Keywords: Compound pendulum, Liquid damping, Small-angle approximation, Oscillation period, Linear correction model.

1. Introduction

Pendulums have long held a prominent role in our everyday lives, particularly within the fields of physics. These devices can be seen in various forms, from the playful swings that bring joy to children to the implementation of tuned mass dampers, which enhance the stability and safety of towering skyscrapers (Heffernan, 2015), and even extend to the field of rocketry, and a dual shock absorber system is employed to ensure the smooth launch by reducing excessive vibrations (Malik, 2008).

In physics education, the simple pendulum is a commonly taught concept (Suzuki, 2008), but scientists have expanded their research to explore the intricacies of compound pendulum systems (Hinrichse, 1981). However, most studies in this area have focused solely on ideal situations without considering the effects of friction (Feynman, 1963). It is important to correct these idealized models and account for damping conditions that can cause non-linear motion and chaos (Ji, Zhou, & Li, 2018), and difficult to calculate and understand (Peters, 2003). By incorporating damping effects, scientists can develop more accurate models and gain a better understanding of the real-world behavior of compound pendulums.

While some researchers have directed their attention toward investigating the effects of air friction on compound pendulums (Zhang, Wang, Qu, & Zou, 2008), an emerging area of interest lies in exploring the influence of liquid damping. By studying the behavior of these systems, we can gain valuable insights into their dynamics and further our understanding of their real-world applications.

When it comes to liquid damping situations, the theoretical calculation of the magnitude of viscous resistance is quite complex, which includes viscosity, mass, length, cross-sectional area, and so on. However, when discussing the effect of fluid damping, two simplified models are commonly used, one assumes that the friction acting on the pendulum is proportional to the velocity, while the other assumes that the friction is proportional to the square of the velocity (Lü, 2006). In this essay, we will calculate the period of compound pendulums with liquid damping using two previous approximation methods and compare the differences between these two methods and experimental results.

2. Derivation

2.1 Liquid friction proportional to velocity

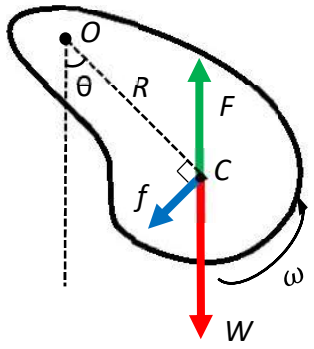

Fig 1. A free body diagram of a compound pendulum

As we can see from Fig.1, assume the pendulum is acted by a gravitational force W, which is fixed at point O and has the center of mass at C. The distance between axes O and C is R, and the angle between the vertical line and OC is θ, while the pendulum is swung at angular velocity ω. Examining the forces acting on the pendulum reveals three components: gravitational force W, buoyance F, accounting for complete liquid submersion, the third is the most important, and the crucial frictional force f. In this situation, it is proportional to velocity, i.e.

$$f = -kv = -kR\omega$$

k here stands for the damping constant of the pendulum, and f is minus since it is opposite to the direction of rotation. According to the analog Newton's Second Law in rotation

$$I\alpha = \sum M \tag{1}$$

R.H.S. is the sum of all the moments, which can be expanded. By substituting all the forces and their moments, equation (1) can be written as

$$I\ddot{\theta} = WRsin\theta + FRsin\theta + fR$$

Expand each term.

$$I\ddot{\theta} = -mgRsin\theta - k\omega R^2 + \rho gVRsin\theta \tag{2}$$

Notice that weight is also opposite to the direction of rotation, so there should be another minus sign before it. Then, (2) can be rewritten in differential form.

$$I\ddot{\theta} + kR^2\dot{\theta} + (m - \rho V)gRsin\theta = 0 \tag{3}$$

For small θ, which $\theta \ll 5°$, we have $sin\theta \approx \theta$. There is a discussion of whether the small angle is possible or not in liquid damping, experiments later will show this problem and prove that it is available.

i.e. (3) can be written in

$$\ddot{\theta} + \frac{kR^2}{I}\dot{\theta} + \frac{(m - \rho V)gR}{I}\theta = 0$$

Let $r_1 = \frac{kR^2}{I}$, $r_2 = \frac{(m-\rho V)gR}{I}$, and

$$\frac{d^2\theta}{dt^2} + r_1\frac{d\theta}{dt} + r_2\theta = 0 \tag{4}$$

This is a homogeneous second-order linear ordinary differential equation. Notice that $\frac{d}{dx}e^{f(x)} = \frac{d}{dx}f(x)e^{f(x)}$, which the nth derivative of $e^{f(x)}$ is $\left(\frac{d}{dx}f(x)\right)^n e^{f(x)}$, original form times a coefficient, we can promote into (4). Assume $\theta = Ae^{mt}$, so $\dot{\theta} = Ame^{mt} = m\theta$, $\ddot{\theta} = m^2\theta$. Substitute into (4)

$$m^2\theta + r_1 m\theta + r_2\theta = 0$$

Each term of the equation has θ, by simplifying it there is

$$m^2 + r_1 m + r_2 = 0$$

This is a linear equation in two unknowns. By finding m we can solve θ, where $\Delta = b^2 - 4ac = r_1^2 - 4r_2$, where $\sqrt{\Delta} = i\sqrt{4r_2 - r_1^2}$, $i = \sqrt{-1}$. According to quadratic formula $x = \frac{-b \pm \sqrt{b^2-4ac}}{2a}$,

$$m = \frac{-r_1 \pm i\sqrt{4r_2 - r_1^2}}{2I}$$

According to Cambridge International AS & A Level Further Mathematics Coursebook, pp. 550-556, if a homogeneous second-order linear ordinary differential equation has roots of auxiliary equation $\lambda_1 = a + bi$, $\lambda_2 = a - bi$, then the complementary form is given by $y = e^{ax}(A\,cos\,bx + B\,sin\,bx)$. i.e.

$$\theta = e^{-\frac{r_1}{2}t}\left[A\,cos\left(\frac{i\sqrt{4r_2-r_1^2}}{2}t\right) + B\,sin\left(\frac{i\sqrt{4r_2-r_1^2}}{2}t\right)\right] \quad (5)$$

This is the solution to (4). The presence of complex numbers in the solution represents the system's behavior in phase space. To get the actual period of the pendulum, we should extract the real part of the function. From DeMoivre's theorem, $cos\,n\theta + i\,sin\,n\theta = (cos\,\theta + i\,sin\,\theta)^n = e^{in\theta}$,

$$cos\left(\frac{i\sqrt{4Ir_2 - r_1^2}}{2}t\right) = e^{\frac{i}{2}\sqrt{4r_2-r_1^2}t} \quad sin\left(\frac{i\sqrt{4Ir_2 - r_1^2}}{2}t\right) = e^{-\frac{i}{2}\sqrt{4r_2-r_1^2}t}$$

i.e.

$$\theta = e^{-\frac{r_1}{2}t}\left[Ae^{\frac{i}{2}\sqrt{4r_2-r_1^2}t} + B\,e^{-\frac{i}{2}\sqrt{4r_2-r_1^2}t}\right]$$

$$= e^{-\frac{r_1}{2}t}\left[(A+B)\;cos\left(\frac{\sqrt{\{4r_2-r_1^2\}}}{2}t\right) + i(A-B)\;sin\left(\frac{\sqrt{\{4r_2-r_1^2\}}}{2}t\right)\right] \quad (6)$$

The real part of (6) is

$$\theta = Ce^{-\frac{r_1}{2}t}\,cos\left(\frac{\sqrt{4r_2-r_1^2}}{2}t\right) \quad (7)$$

This is a cosine function of t, where $Ce^{-\frac{r_1}{2}t}$ is the coefficient and decreases with time. This suits the real action in damping conditions, that as time goes by, the pendulum swings with a smaller and smaller angle, but the time taken for each cycle does not change.

To calculate the period of a trigonometry function, we should first find out the angular frequency, which is ω. Therefore, since the original period of $cos(x)$ is 2π, the current period can be calculated by $T = \frac{2\pi}{\omega}$.

Within (7), $\omega = \frac{\sqrt{4Ir_2 - r_1^2}}{2}$, thus

$$T = \frac{2\pi}{\omega} = \frac{2\pi}{\frac{\sqrt{4r_2 - r_1^2}}{2}} = \frac{4\pi}{\sqrt{4r_2 - r_1^2}}$$

Recall that $r_1 = \frac{kR^2}{I}$, $r_2 = \frac{(m-\rho V)gR}{I}$,

$$T = \frac{4\pi}{\sqrt{4\frac{(m-\rho V)gR}{I} - \frac{k^2R^4}{I^2}}} \tag{8}$$

This is the formula of the condition where the damping force is directly proportional to the velocity.

2.2 Liquid friction proportional to the square of velocity

In the second situation, the friction acting on the compound pendulum is proportional to the square of velocity, that is

$$f = -kv^2 = -kR^2\omega^2$$

Again, k here stands for the damping constant of the pendulum. Hence (2) can be rewritten in

$$I\ddot{\theta} = -mgRsin\theta - k\omega^2R^3 + \rho gVRsin\theta \tag{9}$$

Notice that the second term has been change into $-k\omega^2R^3$, which refers to the moment of the friction acting on the pendulum, where $M = fR = -k\omega^2R^2 \cdot R = -k\omega^2R^3$. This term is also negative because it is in the opposite direction of rotation. Rearrange it into differential form we have

$$I\ddot{\theta} + kR^3\dot{\theta}^2 + (m-\rho V)gRsin\theta = 0 \tag{10}$$

Also, θ is a small angle that $\theta \ll 5°$, as a result, we have $sin\theta \approx \theta$.

$$\ddot{\theta} + \frac{kR^3}{I}\dot{\theta}^2 + \frac{(m-\rho V)gR}{I}\theta = 0$$

Ler$r_1 = \frac{kR^3}{I}$, $r_2 = \frac{(m-\rho V)gR}{I}$, afterwards

$$\frac{d^2\theta}{dt^2} + r_1\left(\frac{d\theta}{dt}\right)^2 + r_2\theta = 0 \tag{11}$$

This represents a second-order non-linear ordinary differential equation, distinct from our previous solution. A new mathematical approach is required due to the presence of a square on the first derivative. Assume $y = \left(\frac{d\theta}{dt}\right)^2$, where is a function about θ. According to

$$\frac{d}{d\theta}y = \frac{d}{d\theta}\left(\frac{d\theta}{dt}\right)^2 = 2\frac{d^2\theta}{dt^2}$$

(11) can be shifted into another differential equation about y.

$$\frac{dy}{d\theta} + 2r_1 y + 2r_2\theta = 0 \tag{12}$$

Here (12) is a linear differential equation. By solving y we can get the function of θ through some extent. However, details still need to be listed due to this is not an easy job. Convert (12) into

$$dy + 2(r_1 y + r_2\theta)d\theta = 0 \tag{13}$$

Let $m = 2(r_1 y + r_2\theta)$, where $dm = 2r_1 dy + 2r_2 d\theta$, and (13) can be transferred into $dy + md\theta = 0$. According to m , $y = \frac{m}{2r_1} - \frac{r_2}{r_1}\theta$. Differentiate y, $dy = \frac{dm}{2r_1} - \frac{r_2 d\theta}{r_1}$. Use instead into (13).

$$\frac{dm}{2r_1} - \frac{r_2 d\theta}{r_1} + md\theta = 0$$

Simplify the equation and we get an integrable expression of dm and $d\theta$.

$$\frac{dm}{2r_2 - 2r_1 m} = d\theta$$

Upon integration, the function m is determined as:

$$m = \frac{A}{e^{2r_1\theta}} - \frac{r_2}{r_1}$$

Take into $y = \frac{m}{2r_1} - \frac{r_2}{r_1}\theta$,

$$y = \frac{A}{e^{2r_1\theta}} - \frac{r_2}{r_1}\theta + \frac{r_2}{2(r_1)^2}$$

Where A is an integral constant. To calculate A, consider when $\theta = \theta_0$, i.e., maximum amplitude, $\frac{d\theta}{dt}\Big|_{\theta=\theta_0} = 0$, along with $y = \left(\frac{d\theta}{dt}\right)^2 = 0$. Through substitution,

$$A = \frac{r_2}{2(r_1)^2}(2r_1\theta_0 - 1)e^{2r_1\theta_0} \tag{14}$$

Now y and A have been worked out, and it should be followed by deriving θ from y, which

$$\frac{A}{e^{2r_1\theta}} - \frac{r_2}{r_1}\theta + \frac{r_2}{2(r_1)^2} = \left(\frac{d\theta}{dt}\right)^2$$

Take the square root of both the LHS and RHS sides. Separate the variables.

$$\sqrt{\frac{A}{e^{2r_1\theta}} - \frac{r_2}{r_1}\theta + \frac{r_2}{2(r_1)^2}} = \frac{d\theta}{dt}$$

Expand and integrate both sides.

$$\int d\,t = \int \left(\frac{A}{e^{2r_1\theta}} - \frac{r_2}{r_1}\theta + \frac{r_2}{2(r_1)^2}\right)^{-\frac{1}{2}} d\theta$$

(15)

From using the Maclaurin series $e^x = \sum_{n=0}^{\infty} \frac{x^n}{n!}$, the approximate value of e can be simply calculated by the first three terms. And

$$e^{-2r_1\theta} = 1 + \frac{(-2r_1\theta)}{1!} + \frac{(-2r_1\theta)^2}{2!} \tag{16}$$

Take into (15), RHS can be exchanged into

$$\int \left(\left(A + \frac{r_2}{2(r_1)^2}\right) - \left(2Ar_1 + \frac{r_2}{r_1}\right)\theta + 2A{r_1}^2\theta^2\right)^{-\frac{1}{2}} d\theta$$

(17)

By completing the square method, notice that

$$\left(A + \frac{r_2}{2(r_1)^2}\right) - \left(2Ar_1 + \frac{r_2}{r_1}\right)\theta + 2A{r_1}^2\theta^2 = \left(\frac{A}{2} - \frac{{r_2}^2}{4(r_1)^4}\right) + (2A)\left(\left(\frac{1}{2} + \frac{r_2}{4(r_1)^2A}\right) - r_1\theta\right)^2$$

And (17) is equivalent to

$$\int \frac{\sqrt{-8A}}{\sqrt{\frac{{r_2}^2}{4(r_1)^4} - A^2}\sqrt{1 - \frac{\left(2Ar_1\theta - \left(A + \frac{r_2}{2(r_1)^2}\right)\right)^2}{\frac{{r_2}^2}{4(r_1)^4} - A^2}}} d\theta$$

(18)

From $\int \frac{1}{\sqrt{1-x^2}} dx = sin^{-1}(x)$, take (18) into (15).

$$\Delta t = -\frac{\sqrt{\frac{-2}{A}}}{r_1} sin^{-1}\left[\frac{2Ar_1\theta - \left(A + \frac{r_2}{2(r_1)^2}\right)}{\sqrt{\frac{{r_2}^2}{4(r_1)^4} - A^2}}\right]$$

(19)

Arrange (19), express θ in t.

$$\theta = \frac{A + \frac{r_2}{2(r_1)^2}}{2Ar_1} - \frac{\sqrt{\frac{{r_2}^2}{4(r_1)^4A^2} - 1}}{2r_1} sin\left[r_1\sqrt{-\frac{A}{2}}t\right] \tag{20}$$

In (20), the angular frequency $\omega = r_1\sqrt{-\frac{A}{2}}$. Recall $A = \frac{r_2}{2(r_1)^2}(2r_1\theta_0 - 1)e^{2r_1\theta_0}$.

$$\omega = r_1\sqrt{-\frac{A}{2}} = r_1\sqrt{-\frac{(2r_1r_2\theta_0 - r_2)e^{2r_1\theta_0}}{(r_1)^2}} = \sqrt{\frac{r_2 - 2r_1r_2\theta_0}{e^{-2r_1\theta_0}}}$$

Refer to (16)

$$\omega = \sqrt{\frac{r_2 - 2r_1r_2\theta_0}{e^{-2r_1\theta_0}}} = \sqrt{\frac{r_2 - 2r_1r_2\theta_0}{1 - 2r_1\theta_0 + 2r_1^2\theta_0^2}}$$

Recall $r_1 = \frac{kR^3}{I}$, $r_2 = \frac{(m-\rho V)gR}{I}$,

$$\omega = \sqrt{\frac{\frac{(m-\rho V)gR}{I} - 2\frac{(m-\rho V)gkR^4}{I^2}\theta_0}{1 - 2\frac{kR^3}{I}\theta_0 + 2\frac{k^2R^6}{I^2}\theta_0^2}} = \sqrt{\frac{(m-\rho V)gR(I - 2kR^3\theta_0)}{I^2 - 2kR^3I\theta_0 + 2k^2R^6\theta_0^2}}$$

and from $T = \frac{2\pi}{\omega}$, the period of oscillation can be calculated directly.

$$T = \frac{2\pi}{\omega} = \frac{2\pi}{\sqrt{\frac{(m-\rho V)gR(I - 2kR^3\theta_0)}{I^2 - 2kR^3I\theta_0 + 2k^2R^6\theta_0^2}}} \tag{21}$$

2.3 Checking and Verifications

In the culmination of our preceding computations, both methodologies have adeptly provided theoretical insights into the period of a compound pendulum influenced by liquid damping under distinct conditions. It is noteworthy that the utilization of approximations in both approaches serves the purpose of streamlining the differential equation into a second-order form. The judicious expansion of

the exponential function is specifically aimed at obtaining an integrable function featuring a periodic component, such as the sin function.

In a general sense, we express the periods T as follows:

1. For the assumption where $f = -kv = -kR\omega$:

$$T = \frac{4\pi}{\sqrt{\frac{4(m-\rho V)gRI - k^2R^4}{I^2}}}$$

2. For the assumption where $f = -kv^2 = -kR^2\omega^2$:

$$T = \frac{2\pi}{\sqrt{\frac{(m-\rho V)gR(I - 2kR^3\theta_0)}{I^2 - 2kR^3I\theta_0 + 2k^2R^6\theta_0^2}}}$$

To assess the accuracy of both formulations, we evaluate the scenarios where $k = 0$ and $\rho gV = 0$, signifying a scenario where the compound pendulum remains devoid of any liquid submersion and friction. Remarkably, in both cases, the derived periods converge to $T = 2\pi\sqrt{\frac{I}{mgR}}$, aligning with the theoretical period for ideal non-energy loss oscillations. This consistency reinforces the validity of our methodology.

An additional scrutiny is applied to the small angle approximation. Both approaches assert that for $\theta \ll 5°, \sin\theta \approx \theta$. However, a critical inquiry arises: can small angles be pertinent in the presence of substantial damping, as encountered in mediums like water, oil, or ethanol? Esteemed researchers (Alciatore & Histand, 2007) introduced a physical quantity δ, signifying the damping ratio where $\delta = \frac{actual\ damping}{critical\ damping}$. Over-damping conditions occur when $\delta > 1$, leading to the absence of observable periodic swings. To avert such scenarios and ascertain the suitability of liquid damping for most pendulums, experiments must be conducted to determine the feasibility of assuming small angles. This empirical validation is essential for refining our models and ensuring their accuracy under real-world conditions.

Moreover, while the two mentioned approximation methods provide distinct approaches for determining the period of a compound pendulum, they do not offer guidance on the preferred choice for predicting the pendulum's motion. For a more comprehensive understanding, additional experiments are imperative. These experiments serve to assess and compare the accuracy of both methods through controlling variables constant and only keeping rotational radius exchanging, thereby enabling the formulation of well-founded conclusions through a meticulous analysis of the experimental outcomes.

3. Experiments

3.1 Rough Experiments

The preceding discussion emphasized the importance of experimental verification, prompting the need to assess the validity of assuming small angles. To tackle this, a rough experiment was carefully designed.

In the experiment, a long screw with a textured surface was chosen to simulate a compound pendulum. The textured surface was intentionally picked to highlight the impact of liquid damping on the pendulum's motion. It is noteworthy that a hole was carefully drilled through the screw to accommodate the axes for support. An iron support was strategically positioned to provide a stable horizontal foundation for the entire system. Copper wire served as the rotation axes, and though occasional loosening could appear, it was expected to have a minimal effect on the pendulum's period.

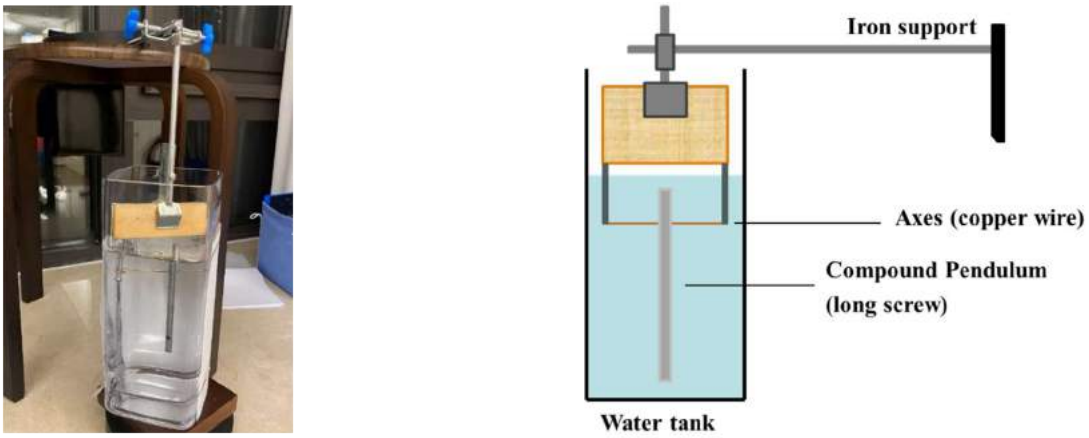

a. pictures from the experimental site b. schematic diagram

Fig 2. Rough Experiment

No.	Equipment Name	Device Model	Role
1	Water tank	12cm * 12cm *25cm	Contain water
2	Iron stand	30cm in length	Provide the horizontal foundation
3	Clamps	Iron with rubber	Hold the entire system
4	Wooden block	15cm * 5cm * 1cm	Support the axes
5	Copper wire	7mm in diameter	Rotational axes
6	Aluminum screw	M8, 121.5mm in length	Compound pendulum
7	Camera	iPhone 11 *0.125 in slow-motion	Record the experiment

Table 1. Equipment list of rough experiments

To enhance measurement precision, the incorporation of cameras and slow-motion technology was employed. Video editing tools were subsequently utilized to tally the frames encompassing a complete oscillation period. Variable control was not implemented since this is an initial stage of validation, resulting in only a singular set of data being amassed. The experimental procedure was repeated four times, with the computation of an average value.

3.2 Formal Experiments

In the formal experiments, a cubic apparatus was designed to serve as a container for masses with diverse weights and densities. This arrangement aimed to alter the compound pendulum's inertia by adjusting the mass center's position. Through this method, the investigation delves into the connection between the oscillation period and the rotational radius of the mass center. Additionally, it enables a comparison of the precision achieved by both approaches.

The creation of this apparatus, requiring qualities of lightness, strength, and waterproofing, involves the utilization of a 3D printer for model fabrication. The chosen materials possess enhanced strength, the ability to adapt shape freely, and the capacity to generate noticeable friction on the pendulum.

a. Container overview

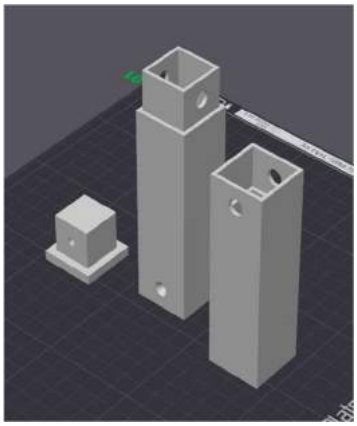

b. Design display [blender]

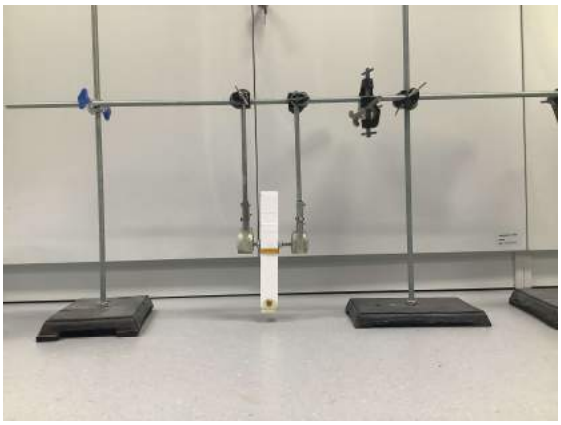

c. Container ready for experiments

Fig 3. Container and design diagram [blender]

The design of the experimental container has been carefully crafted to ensure the ease of inserting and exchanging masses during experimental procedures. A paramount consideration in this design is the necessity for waterproofing, aiming to prevent water ingress that might otherwise induce changes in mass and inertia, thereby potentially impacting the period of the pendulum. A lid is securely affixed at the container's base. Its position is reinforced by two nails and sealed with waterproof paper.

To maintain a balanced mass distribution, the container's main body is divided into two approximately equal halves. A long-threaded M8 rod passes through strategically placed holes on both sides of the walls, serving as the rotational axis. The tight securing of this axis is achieved by nuts and rubber silicone gaskets, and rubber bands are positioned around the slit between the two container halves. Tapes and fasteners are placed to improve the friction between the rotating axis and its supports.

Arranged vertically, three iron stands support a horizontal beam, each standing in a different direction to ensure a stable foundation. Two clamps extend downward from the horizontal beam, firmly securing two bearings. Submerged in liquid, both the container and the axes create an environment of complete fluid

damping. This condition is maintained by placing a substantial water bucket beneath the clamps, ensuring a consistent immersion. The accompanying pictures represent a complete view of the setup, prepared for experiments.

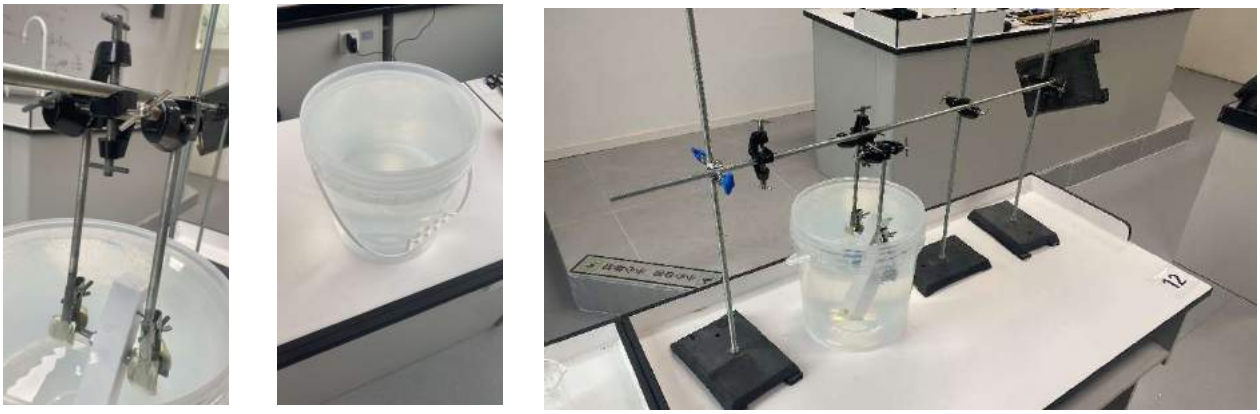

Fig 5. Clamps, water bucket, and an overview

A set of precisely tailored masses is strategically chosen to maintain balance within the container. This decision ensures constancy across all variables throughout the experiments. A mobile phone, equipped with slow-motion video capabilities, aids in capturing convenient calculations of the pendulum's oscillation period.

Over ten experiments are conducted, introducing varying masses for diverse rotational settings. Adobe Effect (AE) is utilized for meticulous frame count tallying, with data systematically logged into a structured table. The experimental equipment is visually depicted in the accompanying figure and detailed in the concise table below for clarity.

No.	Equipment Name	Device Model	Number
1	Mass block	2cm * 1cm in cross-section	9
2	Iron stands	100cm in length	4
3	Clamps	Iron with rubber	2
4	Rod	M8, 10cm in length	2
5	Bearing	10mm in inner diameter	2
6	Silicon gaskets	M8, 1mm in thickness	2
7	Nut	M8, hexagon	2
8	Rubber bands	8cm in original length	1
9	Water buckets	20cm in diameter	1
10	Camera	iPhone 11 *0.125 in slow-motion	1
11	Vanier caliper	15cm max.	1

Table 2. Equipment list

Fig 6. Equipment

4. Analysis

In this segment, unless explicitly specified otherwise, $g = 9.81m\ s^{-2}$.

4.1 Analysis of Rough Experiment

No.	Frame/f	10T/s	T/s
1	740	6.167	0.614
2	736	6.133	
3	732	6.100	
4	738.5	6.154	

Variable	Value	Unit
k	0.84 ± 0.02	$kg\ s^{-1}$
I	0.60 ± 0.003	$g\ m^2$
m	36.0 ± 0.5	g
V	5.00 ± 0.05	ml
R	25.7 ± 0.1	mm

Table 2. Data of rough experiments

The obtained results were organized in a data table to determine the average outcome. However, special consideration was given to the performance during extended continuous swings. Over sixty periods were observed until the pendulum came to a halt, taking more than 40 seconds to complete. Theoretical calculations can also examine the result. The physical quantity δ can be calculated by $\delta = \frac{C}{2m}$ where $m\ddot{x} + C\dot{x} + kx = 0$ (Zhen, Jia, & Fang, 2004). In (4) we have assumed that $\ddot{\theta} + r_1\dot{\theta} + r_2\theta = 0$, leads to $\delta = \frac{r_1}{2} = \frac{kR^2}{2I}$. Take the data below into it, $\delta = 0.15 < 1$, which is not over-damped. As a result, both observation and theories supported the notion that small angles could be reliably used as an approximation under conditions of liquid damping.

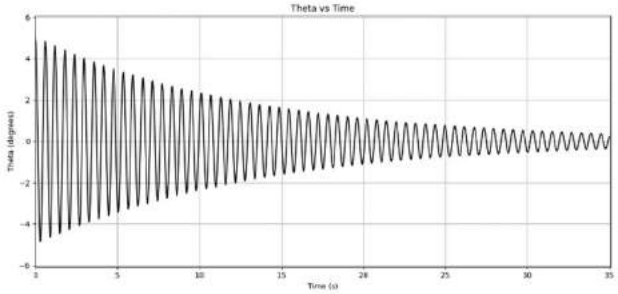

$\frac{\theta}{^\circ}$ about $\frac{t}{s}$ from 0s to 30s

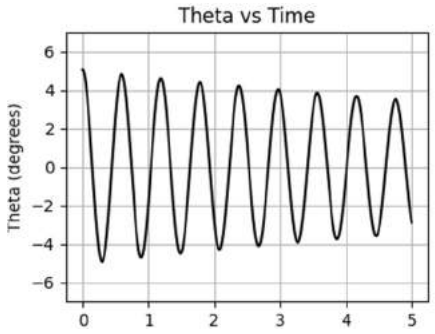

$\frac{\theta}{^\circ}$ about $\frac{t}{s}$ from 0s to 5s

Fig 7. Curves of θ about t [python]

While the primary goal of this rudimentary experiment was to confirm assumptions regarding small-angle considerations, there is potential for additional calculations to be conducted. Taking all the variables, throughout the first method can get $T_1 = 0.60 \pm 0.04\ s$. Simultaneously, the outcome of the second method is $T_2 = 0.58 \pm 0.06\ s$. Notably, the results exhibit only a $\pm 5\%$ deviation from the actual value, affirming the accuracy of both formulas concurrently.

4.2 Analysis of Formal Experiment

With a total mass of 110.70 grams and a volumetric capacity of 185.0 milliliters, the container stands at an overall height of 20.55 centimeters. Its halves, each measuring ten centimeters in length, feature square-shaped cross-sections with sides of three centimeters. Within each half, a confined space unfolds, defined by square cross-sections, each side measuring two centimeters.

The following table presents fundamental data concerning nine distinct masses distributed across three different materials. It is important to note that the provided information is derived from measurements rather than predetermined parameters.

No.	material	A/cm^2	h/cm	V/ml	m1/g	m2/g	m3/g	m/g
1	plastic	2.00	2.82	5.64	7.78	7.76	7.76	7.77
2		2.00	4.00	8.00	10.97	10.98	11.02	10.99
3		2.00	4.68	9.36	11.47	11.48	11.47	11.47
4	Al	2.00	3.34	6.68	16.63	16.63	16.63	16.63
5		2.00	4.32	8.64	22.10	22.08	22.08	22.09
6		2.00	5.34	10.68	27.64	27.64	27.62	27.63
7	Fe	2.00	3.14	6.28	46.26	46.25	46.27	46.26
8		2.00	4.48	8.96	61.89	61.90	61.90	61.90
9		2.00	5.28	10.56	77.92	77.95	77.95	77.94

Table 4. Table of masses

Furthermore, four blocks are selected for placement within the container, each positioned strategically to alter the rotational radius. The recorded periods are listed below.

No.	R/cm	F1/f	F2/f	F3/f	T1/s	T2/s	T3/s	T/s
1	7.96	290	292	284	1.208	1.217	1.183	1.203
2	7.67	226	232	244	0.941	0.965	1.017	0.974
3	5.76	192	209	199	0.802	0.872	0.828	0.834
4	5.00	465	425	448	1.939	1.772	1.866	1.859
5	4.28	227	223	223	0.946	0.929	0.929	0.935
6	3.92	222	219	222	0.925	0.913	0.925	0.921
7	3.50	107	107	105	0.448	0.446	0.438	0.444
8	3.13	258	252	246	1.075	1.050	1.025	1.050
9	2.41	318	295	301	1.325	1.229	1.254	1.269
10	1.50	361	368	378	1.503	1.533	1.575	1.537
11	1.05	439	451	451	1.831	1.879	1.879	1.863

Table 5. Table of Recordings

Here, F1, F2, and F3 are the number of frames counted in the video editor, where one frame equals $\frac{1}{240} \approx 4.16ms$, and T1, T2, and T3 are the time measured from the frame, respectively.

Quantify the discrepancies using Python and the `Matplotlib` library to create a graphical representation. This graph will facilitate the comparison of divergences between experimental outcomes and the two methods utilized. To enhance precision, extend the analysis to various friction constants.

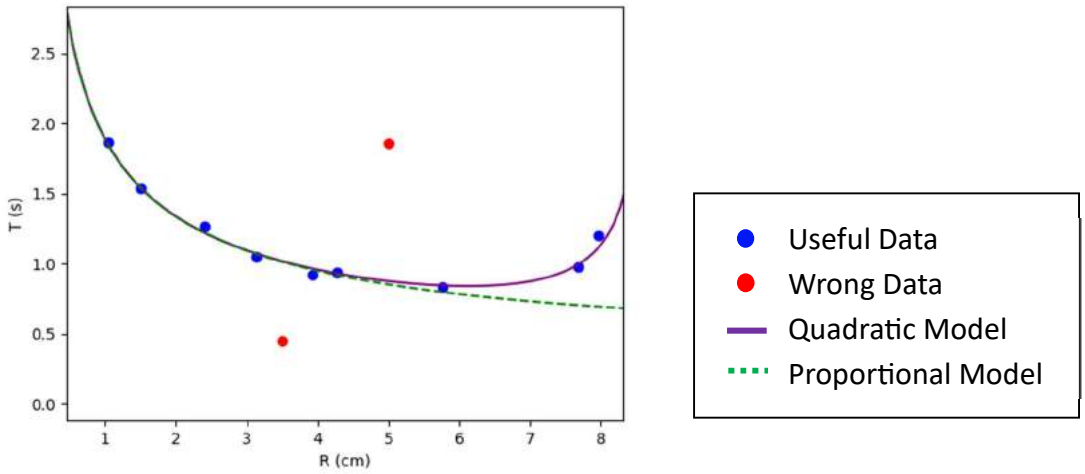

Fig 8. Curves of t about R [python]

Based on the experimental data, two sets out of the eleven recorded exhibit substantial discrepancies, prompting their exclusion from subsequent calculations. Employing the functionalities of the `numpy` and `scipy` libraries, curve fitting in Python becomes an accessible task. The computation yields a value for k of $0.5\ kg\ s^{-1}$, aligning seamlessly with the data obtained during experimentation. Simultaneously, by employing programming tools to assess the variance between experimental and theoretical values, we gain valuable insights into the most appropriate methodology to adopt.

Organizing the initial four datasets in ascending order, the `var()` function efficiently computes the variance across various models and data. Notably, the proportional model demonstrates a slightly reduced variance, underscoring its heightened reliability.

```
Variance of squared model: 0.0007568985124692573
Variance of proportional model: 0.0007271175137054576
```

Fig 9. Log of the program using the first four sets of data [python]

Applying the same analytical approach to the latter four datasets, the program unveils a similar trend. Specifically, the squared model displays a marginally smaller variance.

```
Variance of squared model: 0.0018846709393863 26
Variance of proportional model: 0.040221857184667864
```

Fig 10. Log of the program using the last four sets of data [python]

The initial four datasets show small rotational radii, while the last four exhibits the opposite trend. This suggests that a first-order model effectively corrects the oscillation period when the suspension point is near the center of mass. Conversely, a second-order model is more suitable when the suspension point is farther from the center of mass.

4.3 Theoretical analysis

While conclusions have been drawn, the slight disparity in variance under a small radius state does not strongly support the adoption of the proportional model. Consequently, additional simulations are essential to assess the requisite application of models for stabilizing the oscillation period of a compound pendulum affected by liquid damping. This necessitates exploring variations in the friction constant.

From the previous experiments, $k = 0.5kg\ s^{-1}$. Keep other variables constant, where $V = 184.95ml$, $m = 258.82g, \theta = 5°$, only changing k from 0 to 2.5.

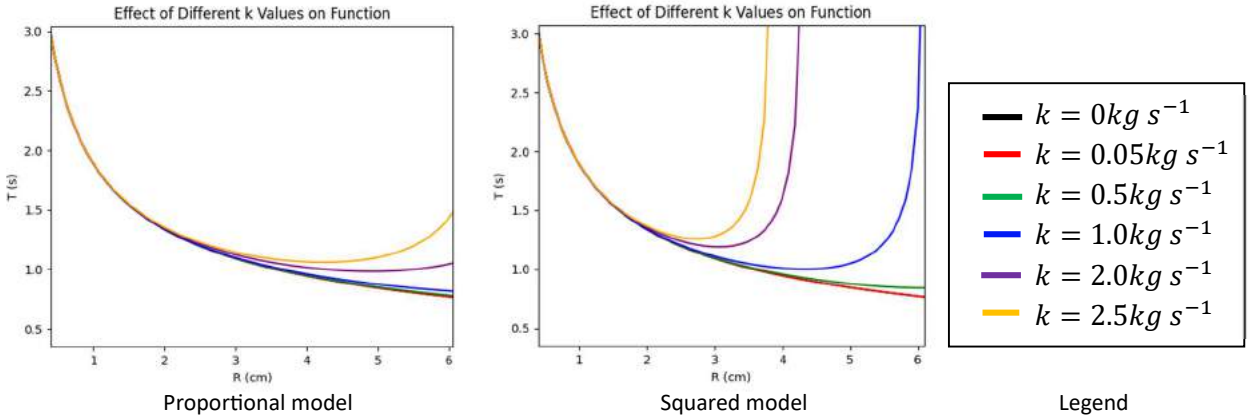

Proportional model Squared model Legend

Fig 11. Effects of k on the period about radius [python]

The picture illustrates theoretical simulations depicting different resistant constants. Notably, in the squared model, as the radius increases, the period extends infinitely. This implies unreliability when both the constant and radius are large, but we need to notice that those values of friction constant are almost impossible. Furthermore, in situations characterized by low damping ($k < 0.5kg\ s^{-1}$), there is a lack of pronounced disparities between the two methods when compared to the ideal scenario. Specifically, when $k = 0.05kg\ s^{-1}$, its curve closely aligns with the ideal curve. This emphasizes the subtle impact of damping on the oscillatory behavior of the system.

Generally, in small friction and a large radius condition, the squared model may exhibit higher precision. What is more, when considering factors such as the complexity of formula derivations and the time required for calculations in environments without computer assistance, it is recommended to choose the proportional model under a small radius condition.

4.4 Error and accuracy analysis

During experiments, variations may occur, affecting outcomes. While acceptable in initial hypothesis tests, caution is necessary in formal research. Inadvertent human errors notably compromised data integrity, as seen in the divergence of two unusable data sets.

Within the subset of results exhibiting a lower magnitude, the oversight of neglecting to secure a rubber band proved pivotal. This oversight allowed water to infiltrate the inner walls of the container, augmenting its mass and consequently reducing the measured rotational period. Conversely, the set of results displaying a higher magnitude is directly attributable to a wrong-adjusted weighting mechanism. In this instance, the misplacement of a plastic block instead of an aluminum block led to a decrease in mass. Thus, the gravitational force became insufficient to balance buoyance, resulting in a naturally inclined state, as illustrated in the accompanying diagram.

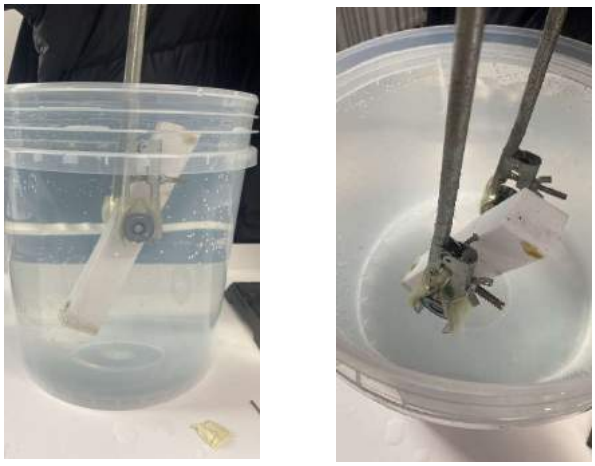

Fig 12. Buoyance higher than weight

In experimentation, uncertainties persist, notably in situations like the excessive rotation of a large-radius axis, exemplified by the M8 screw, causing fluid resistance. Despite the screw's grooves reducing resistance compared to a simple rod, the overall impact is challenging to quantify. Additionally, assessing lateral sliding resistance in the compound pendulum proves difficult due to its distinct calculation method for frontal force reception.

Moreover, water's fluidity and viscosity pose challenges. Hence, our approach relies on practical measurements for determining resistance constants, lacking precise control over this physical parameter.

5. Conclusion and Reflection

5.1 Conclusion

Drawing upon the insights garnered from prior research and essays, two distinct methodologies have been identified for calculating and correcting the vibrational period of a compound pendulum under the influence of liquid resistance. Through theoretical derivation, we have formulated an expression to compute the corrected period.

In consideration of the feasibility of observing small angles, a rudimentary experiment was devised. Employing a simple apparatus, it was observed that small-angle oscillations were perceptible to the naked eye and exhibited sustained motion over an extended duration. This substantiates the viability of small-angle oscillations of the compound pendulum under liquid resistance, leading to the conclusion that θ can be employed as a direct approximation for $sin\,\theta$. Subsequent calculations further indicated that, under liquid resistance, the compound pendulum's small-angle periodic motion does not experience over-damping, which aligns with experimental expectations.

Subsequently, a formal experiment was conducted, providing a preliminary comparison and discussion of the accuracy of the two correction models. Considering the malleability of 3D-printed materials and the influence of observable friction, a cuboid container was designed. This facilitated the manipulation of variables by altering internal mass and its positioning to control the center of gravity, allowing for an exploration of the relationship between rotational radius and period. Python, Excel, and demos were utilized for data analysis, fitting, computation, and graphical representation. Leveraging these tools enabled a nuanced evaluation of the precision in period calculations between the two models, leading to the conclusion that a linear model should be adopted for smaller radii, while a squared model is more suitable for larger radii.

Finally, numerical calculations were performed using programming, and observations were made through graphical analysis. Gradually increasing the resistance constant revealed that, for $k < 0.5\ kg\ s^{-1}$, the corrected results closely align with the ideal scenario, indicating minimal damping effects on the compound pendulum, which can be directly using the ideal formula. As resistance becomes larger, the squared model demonstrates superior accuracy.

In summary, considering the complexity of computational duration and formula derivation, this essay recommends its use for approximations in a small radius of rotation, despite the slight deviations it may introduce. Moreover, when it comes to the rotational length of the mass center near the length of the pendulum, the squared model seems more accurate.

5.2 Reflection and acknowledgement

Upon reflecting on my entire research, I noticed some areas that could be improved in my first independent scientific exploration.

Firstly, I faced challenges in the theoretical calculation part due to a lack of solid mathematical groundwork. This resulted in repeated deviations and issues during the deduction process, causing delays in my research plan and progress. The use of differential equations, which involves some advanced math, exceeded my current abilities, and took a month for confirmation.

Secondly, the experimental design fell short of achieving the desired goals. Originally, I intended to explore the relationship between periodicity and resistance coefficients, along with rotational radius. However, due to equipment shortages, I had to omit experimenting with different liquids and only conducted experiments in water. When analyzing changes in resistance coefficients, I relied solely on software for feasibility assessments, lacking empirical evidence. Consequently, the conclusions drawn in this paper are preliminary and should be viewed as initial insights.

Thirdly, there were notable errors during experimentation. While not explicitly reflected in the data, this paper simplifies the calculation of resistance coefficients, introducing imprecision. Mistakes during experimentation rendered two out of ten sets of data unusable. Moreover, the limited data sets fail to sufficiently support the drawn conclusions.

In conclusion, this research project served as a valuable learning experience, guiding me through the scientific inquiry process—from initial curiosity to literature review, theoretical calculations, rough and formal experiment design, execution, learning and using modeling and programming software, to data analysis, synthesis, and reflection. I extend sincere thanks to my mentor for guidance, the physics faculty for encouragement, the school laboratory for support, and my parents for their valuable advice.

6. References

Alciatore, D. G., & Histand, M. B. (2007). *Introduction to Mechatronics and Measurement (3rd ed.).*

Feynman, R. P. (1963). *The Feynman Lectures on Physics (Volume I).* California.

Heffernan, T. (2015, March 18). *The World's Second-Tallest Building Sways, But Here's Why You Can't Feel It*. Retrieved December 3, 2023, from Popular Mechanics: https://www.popularmechanics.com/technology/infrastructure/a14564/the-121-story-tower-that-never-sways/

Hinrichse, P. F. (1981, May). Practical Applications of the Compound Pendulum. *The Physics Teacher*, pp. 286-292. Retrieved December 3, 2023

Ji, P., Zhou, L., & Li, L. (2018). Chaotic Motions for a Class of the Compound Pendulum System. *International Conference on Applied Mathematics, Modeling and Simulation (AMMS).* Hangzhou.

Lü, J. (2006). *University Physics Concise Tutorial.* Beijing: Tsinghua University Press.

Malik, T. (2008, August 20). *Shock Absorber Plan Set for NASA's New Rocket*. Retrieved Decemeber 3, 2023, from Space: https://www.space.com/5746-shock-absorber-plan-set-nasa-rocket.html

Mckelvey, L., & Crozier, M. (2018). *Cambridge International AS & A Level Further Mathematics Coursebook.* Cambridge: Cambridge University Press.

Peters, R. D. (2003). Nonlinear Damping of the 'Linear' Pendulum. *arXiv: Classical Physics*. Retrieved 12 3, 2023, from https://arxiv.org/abs/physics/0306081

Suzuki, M. &. (2008). Physics of simple pendulum.

Zhang, T., Wang, Y., Qu, G., & Zou, D. (2008, November). Influence of air resistance on the vibration period of compound pendulum. *Physics Experimentation, 28*(11), 42-45. Retrieved December 4, 2023

Zhen, Y., Jia, Q., & Fang, X. (2004). *Mechanics.* Beijing: Higher Education Press.